

# Variation of resonance-radiation polarization due to self-induced dichroism in a KCl:Li crystal with $F_A$ centers

S. A. Boiko, M. I. Dykman, M. P. Lisitsa, V. I. Sidorenko, and G. G. Tarasov

(Received 3 January 1984)

Opt. Spektrosk. 58, 1055-1058 (May 1985)

The variation of the polarization of elliptically polarized light propagation in a cubic crystal of KCl with reorientable color centers [ $F_A$ (Li) centers] is investigated. It is shown that the change of the polarization ellipse due to the self-induced dichroism leads to a rotation of its semi-major axis toward one of the central symmetry axes of the  $\langle 100 \rangle$  type and to an increase of its eccentricity. A theoretical analysis of the observed effect is carried out.

1. The propagation of radiation in a crystal is accompanied by a variation of its polarization in a number of cases. Such variation is usually a manifestation of the optical anisotropy of the crystal. If the intensity of the radiation is sufficiently large, then the change of the polarization can become self-induced. The self-induced anisotropy for transparent isotropic media is revealed in the fact that the polarization ellipse of the intense radiation is rotated.<sup>1</sup> The variation of the polarization in crystals, generally speaking, has a more complicated character. As is shown in Ref. 2, the polarization ellipse in transparent nongyrotropic crystals is rotated only at specific orientations of the polarization ellipse relative to the crystal axes and at a sufficiently large ellipticity of the incident radiation. In the opposite case the propagation of radiation may be accompanied by spatial oscillations of the polarization; both the tilt angle of the polarization ellipse as well as the degree of ellipticity oscillate.

A relatively large self-induced dichroism<sup>3</sup> takes place on resonance excitation of an impurity electronic transition in cubic crystals with anisotropic color centers. Such dichroism leads to a large self-induced rotation of the plane of polarization (SRPP) of linearly polarized radiation as well as to a rotation and deformation of the polarization ellipse in the case of elliptical polarization of the radiation.

2. Crystals of KCl:Li with  $F_A$  centers were selected for an experimental study of the variation of the radiation polarization because a large SRPP effect is observed in these systems<sup>3</sup>; rotation angles  $> 40^\circ$  have been obtained in nonlaser fields, i.e., in modern terminology, the optical nonlinearity was gigantic.

The apparatus for the study of the interaction of elliptically polarized light with a crystal consisted of a LG-72, He-Ne laser ( $\lambda = 6328 \text{ \AA}$ ), a  $\lambda/4$  plate, a nitrogen contact cryostat in which the object being studied was placed, an analyzer, a photomultiplier, amplifier, and a chart recorder. The analyzer was rotated with constant speed, and the position of the axes and eccentricity of the polarization ellipse were determined from the signal recorded on the recorder.

The KCl:Li ( $\sim 5 \times 10^{-4}$ – $10^{-3}$  mole/mole) crystals were colored radiatively by a dose of 20 Mrad ( $\text{Co}^{60}$ ). The  $F_A$  (II) centers in the crystals were created by the usual method of photodissociation of  $F$  centers.<sup>4</sup> The measurements of the SRPP were carried out at a temperature  $\sim 100 \text{ K}$  on samples of 5–10-mm thickness. The samples of a rightangle shape

were cut off along the  $(100)$  planes. Light was propagated along the  $[001]$  direction. The area of the light spot on the front face of the sample was  $\sim 1 \text{ mm}^2$ .

Experimental studies with elliptically polarized light were made quite difficult by the nonuniformity of the samples and the cryostat windows. The nonuniformity of the cryostat windows was caused by weak birefringence due to mechanical stresses which form on pumping the cryostat and filling it up with liquid nitrogen. The nonuniformity of the samples is connected with their block-like shape, in particular, with the nonuniformity of the distribution of color centers along the crystal.

3. For the model of centers taken in Ref. 3, while neglecting the absorption of the main crystal in the region of the resonance impurity absorption, one can write Maxwell's equations for a slowly varying amplitude of the field  $E$  in the steady-state region in the form

$$(\mathbf{k} \cdot \nabla) E = 2\pi i [k^2 P - \mathbf{k}(\mathbf{k} \cdot \mathbf{P})], \quad (1)$$

where  $\mathbf{k}$  is the wave vector and  $k^2 = \omega^2 \epsilon / c^2$ . One can write the contribution of impurities to the polarization  $\mathbf{P}$  of the crystal, according to Ref. 5, as

$$\mathbf{P} = \frac{\chi}{2\pi k} \sum_n [d_n (d_n E) \rho_n(E) / (f d^2)]; \quad |\chi| \ll k, \quad d^2 = |d_n|^2. \quad (2)$$

Here  $\chi$  is the resonance contribution of the impurity to the complex refractive index in the absence of a resonance optical orientation of the impurity;  $\rho(E_n)$  is the field-dependent relative population of the orientation  $n$  ( $\sum_n \rho_n = 1$ );  $f$  is the normalization parameter ( $f = \sum_n d^2 n_j / d^2$ ;  $j = x, y, z$ );  $d_n$  is the dipole moment of the nondegenerate transition in the  $n$ th orientation; the unit vector  $\mathbf{n}$  is oriented along one of  $x, y$ , or  $z$  axes.

The optical orientation of the tunnel centers is described by the equation of balance<sup>3</sup>

$$\frac{\partial \rho_n}{\partial t} = \sum_m (C_{mn} \rho_m - C_{nm} \rho_n). \quad (3)$$

The coefficient  $C_{nm}$  has the form

$$C_{nm} = B d^2 [|E_n|^2 + \chi (|E|^2 - |E_n|^2)], \quad E_n = (\mathbf{E} \cdot \mathbf{n}), \quad |E|^2 = \sum_n |E_n|^2. \quad (4)$$

under sufficiently weak fields when the population of the excited state is small.

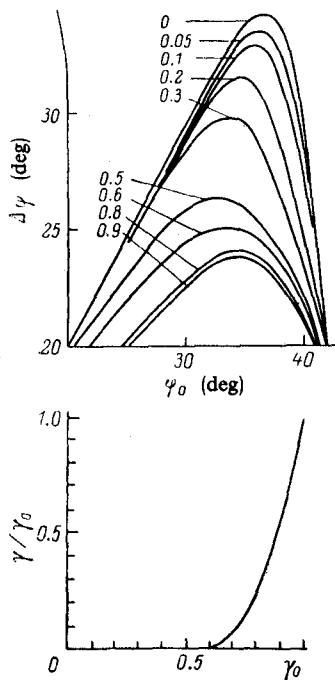


FIG. 1. Theoretical dependence of  $\Delta\varphi_0$  on various values of the parameter  $\Delta\varphi_0$ . The lower part of the figure is the theoretically calculated relative change of the ratio of the semi-axes of the ellipse at the exit of the crystal to that at the input.

The parameter  $\chi$  takes into account the breakdown of the polarization selection rules in the model of the  $\langle 100 \rangle$  centers<sup>4</sup> for a nondegenerate  $F_{AI}$  transition.

For waves propagating along the  $[001]$  direction, we obtain

$$\frac{\partial E_n}{\partial z} = \frac{ixE_n}{1+2\chi} [p_n(1-\chi) + \chi], \quad n = x, y. \quad (5)$$

In the case of elliptical polarization and at exact resonance (when the radiation frequency falls in the center of the  $F_{AI}$  band), the phase difference of the field components is constant; however, the degree of ellipticity of the radiation varies because the ratio

$$|E_y(z)|/|E_x(z)| \equiv |E_y(z)|/|E_x(z)| \equiv \tan \Phi.$$

changes.

The eccentricity  $\varepsilon(z)$  and angle  $\varphi(z)$  between the major axis of the polarization ellipse and the  $[100]$  direction of the crystal are determined by the expressions<sup>6</sup>

$$\varepsilon(z) = [2\sqrt{1 - \sin^2 2\Phi \sin^2 \Psi_{xy}} / (1 + \sqrt{1 - \sin^2 2\Phi \sin^2 \Psi_{xy}})]^{1/2},$$

$$\varphi(z) = \frac{1}{2} \arctan(\tan 2\Phi \cos \Omega_{xy}); \quad \Psi_{xy} = \ln \left( \frac{E_x/E_{x0}}{E_y/E_{y0}} \right),$$

$$E_{x,y} \equiv E_{x,y}(z); \quad E_{x0,y0} \equiv E_{x,y}(0). \quad (6)$$

Integrating Eq. (5), one can easily obtain an expression for the angle

$$\left( \frac{\tan 2\Phi}{\tan 2\Phi_0} \right)^{(1+\chi/2)} \left( \frac{\cos 2\Phi}{\cos 2\Phi_0} \right)^{-(1-\chi)^2/8\chi} = \exp \left[ -\frac{1}{2} (1-\chi)^2 l \right], \quad (7)$$

where  $\tilde{l}$  is the dimensionless thickness of the crystal,  $\tilde{l} = \kappa''/l(1+2\chi)$  ( $l$  is the crystal thickness).

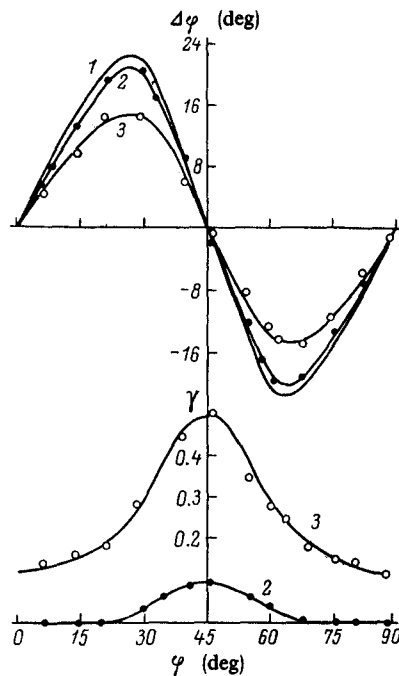


FIG. 2. Variation of the angle formed by the semi-major axis of the polarization ellipse with the  $[100]$  axis of the crystal for various eccentricities of the radiation at the input. Curves 1-3 correspond to values of the parameter  $\gamma_0 = 0, 0.1, 0.5$ . The lower part of the figure is the change of the ratio of the semi-axes of the polarization ellipse at the exit of the crystal on the parameter  $\gamma_0$ .

By numerically solving the transcendental Eq. (7) with the parameters  $\lambda$  and  $\tilde{l}$  determined from experiments on the SRPP for linearly polarized radiation ( $\chi = 0.04$ ), the theoretical dependences of the tilt angle of the semi-major axis of the polarization ellipse to the  $[100]$  axis and the ratio of its semi-axes  $a$  and  $b$  ( $\gamma = b/a, a > b$ ) at the exit of the crystal on the corresponding parameters of the radiation at the input (Fig. 1) were obtained. Let us mention the interesting behavior of the position of the maximum of the function  $\Delta\varphi(\varphi_0)$  at different  $\gamma_0$  (the value of  $\gamma$  at the input of the crystal). This special feature is associated with the fact that the polarization ellipse of the radiation is not only turned in the crystal but also collapses (the radiation is more strongly linearized in proportion to the approach of the semi-axis of the ellipse to the  $[100]$  axis).

In this case when the radiation is close to circularly polarized ( $\gamma_0 \rightarrow 1$ ), the linearization of the radiation practically does not occur (see Fig. 1); however, the semi-major axis of the polarization ellipse is turned by large angles, which depend weakly on  $\gamma_0$  in a certain interval of values of the latter determined by  $\tilde{l}$ .

Theoretical curves calculated at  $\chi = 0.04$  and  $\tilde{l} = 16$  for three different eccentricities of the polarization ellipse of radiation at the input of the crystal are shown in Fig. 2. Let us mention that the experimental results (the points) are described satisfactorily theoretically under the chosen values of the parameters.

We note in conclusion that the scatter of the experimental points depends essentially on the quality of the sample,

the degree of its nonuniformity, and the diameter of the light spot on the front face of the crystal, which limits somewhat the potential of the application of crystals with reorientable centers as various polarizing optical elements.

<sup>1</sup>P. D. Maker, R. W. Terhune, and C. M. Savage, *Phys. Rev. Lett.* **12**, 507 (1964).

<sup>2</sup>M. I. Dykman and G. G. Tarasov, *Fiz. Tverdozo. Tela* **24**, 2396 (1982)

[*Sov. Phys. Solid State* **24**, 1361 (1982)].

<sup>3</sup>M. Ya. Valakh, M. I. Dykman, M. P. Lisitsa, G. Yu. Rudko, and G. G. Tarasov, *Solid State Commun.* **30**, 133 (1979).

<sup>4</sup>F. Luty, in *Physics of Color Centers*, Ed. W. B. Fowler (Academic P., New York, 1968).

<sup>5</sup>M. I. Dykman and G. G. Tarasov, *Zh. Eksp. Teor. Fiz.* **74**, 1061 (1978) [*Sov. Phys. JETP* **47**, 557 (1978)].

<sup>6</sup>M. Born and E. Wolf, *Principles of Optics* (Pergamon P., New York, 1970; Moscow, 1973).

## Low-temperature luminescence and formation of radiation-induced defects in RbI single crystals

V. G. Plekhanov and V. V. Shepelev

(Received 3 January 1984)

*Opt. Spektrosk.* **58**, 1059–1063 (May 1985)

Luminescence and induced absorption spectra of RbI single crystals under x-ray and photoexcitation have been studied in the 4.2–100-K temperature range. In all cases, bands due to radiative annihilation of autolocalized excitons are present in the spectra. Analysis of results of thermostimulated luminescence, fractional bleaching, and annealing of induced absorption indicates a predominant formation of the Frenkel F–H pair during the nonradiative decay of an exciton.

### INTRODUCTION

Many researchers have been concentrating their attention on the distinctive characteristics of intrinsic electronic excitation of alkali halide crystals (AHC), foremost among which should be mentioned the existence of free and autolocalized excitons<sup>1,2</sup> and exciton decay during relaxation to structural defects.<sup>3</sup> The study of intrinsic electronic excitation of AHC makes it possible not only to account for the possible channels of excitation relaxation, but also to establish the mechanisms of the processes involved.<sup>4–9</sup>

In the indicated sense RbI crystals are a convenient subject of study. In the luminescent properties of these crystals, as in those of other AHC,<sup>1,2</sup> manifested the states of free and autolocalized excitons separated by a potential barrier.<sup>10</sup> What is also important is that these crystals are characterized by processes of radiation-induced formation of structural defects (as for example in Ref. 11). Thanks to precisely such a combination of properties, the study of the mechanisms of defect formation by low-energy electronic excitation in RbI is of definite interest.

The aim of this work was to determine the characteristics of the process of formation of Frenkel defects in RbI during nonradiative decay of excitons. For this purpose, we studied the x-ray luminescence (XL), photoluminescence (PL), and tunnel (TL), photostimulated (PSL) and thermostimulated (TSL) luminescence, as well as induced optical absorption and annealing of radiation-induced defects at low temperatures (from 4.2 to 100 K). In particular, the spectra and the TL and TSL kinetics of RbI crystals were measured for the first time, and the predominance of the process of

formation of a Frenkel F–H pair during exciton decay was demonstrated, along with the possibility of formation of an *I* center on capture of an electron by an *H* center.

### SUBJECT AND METHOD OF STUDY

We studied plates of RbI single crystals grown by Stockbarger's method from a raw material purified by zone melting, with fresh spalls on the working surfaces.

The spectral studies were done with an arrangement described previously (for example, in Refs. 7, 10, and 12), using a high-transmission helium immersion cryostat. The induced absorption was also measured with a Specord UV-VIS spectrophotometer. The sample used in the TSL studies was heated at a rate of 0.3–0.5 K/min.

### EXPERIMENTAL RESULTS

In low-temperature XL [Fig. 1(a)] and PL spectra during excitation of exciton absorption in the long-wavelength band [Fig. 1(b)] of RbI single crystals, there are three well-known emission bands with peaks at 3.9, 3.0, and 2.3 eV.<sup>13–16</sup> The strength of the 3.9-eV emission band at  $E_{\text{exc}} = 5.76$  eV is more than two orders of magnitude below the strength of the 3.0-eV band. All the crystals studied are characterized by the presence of emission bands of free excitons in the edge luminescence (Fig. 1., inset<sup>12</sup>). After the x-ray excitation, a long afterglow—TL—is observed. Its spectrum [Fig. 1(c)] also contains three emission bands, but in contrast to XL and PL, one of them has a maximum at 3.25 eV. Figure 1(d) shows the PSL spectrum at 4.2 K, observed during illumination in the absorption band of *F'* centers ( $E_{\text{exc}} = 1.2$  eV<sup>17</sup>) of